J|A|C|S
ARTICLES
Published on Web 03/17/2006

# Single-Site Homogeneous and Heterogeneized Gold(III) Hydrogenation Catalysts: Mechanistic Implications

Aleix Comas-Vives,[⊥] C. González-Arellano,[†,§] A. Corma,*[,‡] M. Iglesias,[§] F. Sánchez,[†] and Gregori Ujaque*[,⊥]

*Contribution from the Instituto de Química Orgánica General, CSIC, C/ Juan de la Cierva 3, 28006 Madrid, Spain, Instituto de Tecnología Química, UPV-CSIC, Universidad Politécnica de Valencia, Avenida de los Naranjos s/n, 46022 Valencia, Spain, Instituto de Ciencia de Materiales de Madrid, CSIC, C/Sor Juana Inés de la Cruz s/n, Cantoblanco, 28049 Madrid, Spain, and Unitat de Química Física, Departament de Química, Universitat Autònoma de Barcelona, 08193 Bellaterra, Barcelona, Catalonia, Spain*

Received November 24, 2005; E-mail: acorma@itq.upv.es; Gregori.Ujaque@uab.es

***Abstract:*** Au(III)−Schiff base complexes are active hydrogenation catalysts, giving turnover frequencies similar to those of the corresponding complexes of Pd(II), which has the same $d^8$ electronic structure as Au(III). The mechanism of the reaction has been studied in detail by a combination of kinetic experiments and theoretical calculations. It is predicted and tested that the nature of the solvent plays a critical role for the heterolytic cleavage of $H_2$ (controlling step). Taking this into account, and by properly selecting the nature of solid supports (polarity and proton-donating ability), it was possible to strongly increase the activity of the homogeneous Au(III) and Pd(II) catalysts by grafting them onto the surface.

## Introduction

Gold catalysis in homogeneous and heterogeneous systems is a matter of increasing interest, owing to the unique properties of this metal for a continuously increasing number of reactions. Following the work of Bond and Sermon,[1] Hutchings,[2] and Haruta et al.,[3] gold has appeared as an interesting catalyst when in the form of salts, gold complexes, and gold supported on different carriers.[4−13] In this way, gold has been successfully used in catalyzing reactions such as CO oxidation at low temperature,[8−10,13] the water−gas shift reaction,[14] decomposition of $NO_x$ with hydrocarbons,[15] selective hydrogenations,[16] carbon−carbon bond formation,[17−20] selective oxidations,[21−25] enantioselective asymmetric aldol condensation,[26] and enantioselective hydrogenation of olefins and imines[27] among others.[28] In the case of heterogeneous catalysis, different hypotheses have been put forward to explain the nature of the gold active sites involved, especially in the case of CO oxidation. In some cases the high activity of gold is associated with negatively charged gold,[29] while in other cases it is claimed that the activity of gold nanoparticles is rather related to atoms bearing a positive density of charge.[9−11,30] Catalysis by gold transition metal complexes can help to elucidate the nature of the active sites for a particular reaction since these can be perfectly characterized and analogies with solid catalysts can be established. We believe that Au(I) and Au(III) species are stabilized on supported gold nanoparticles and they can act as active species.[18] Furthermore, Pd(II) and Au(III) have the same $d^8$ electronic structure, and therefore they may behave similarly, at least for some reactions.

Here we present our findings that Au(III) complexes are able to hydrogenate olefinic molecules with high turnover frequencies

[†] Instituto de Química Orgánica General, CSIC.
[‡] Universidad Politécnica de Valencia.
[§] Instituto de Ciencia de Materiales de Madrid, CSIC.
[⊥] Universitat Autònoma de Barcelona.

(1) Bond, G. C.; Sermon, P. A. *Gold Bull.* **1973**, *6*, 102.
(2) Hutchings, G. J. *Gold Bull.* **1996**, *29*, 123.
(3) Haruta, M.; Tsubota, S.; Kobayashi, T.; Ijima, S. *J. Catal.* **1989**, *115*, 301.
(4) Dyker, G. *Angew. Chem., Int. Ed.* **2000**, *39*, 4237 and references therein.
(5) Corma, A.; García, H. *Chem. Rev.* **2003**, *103*, 4307.
(6) Yao, X.; Li, Ch.-J. *J. Am. Chem. Soc.* **2004**, *126*, 6884.
(7) Wei, Ch.; Li, Ch.-J. *J. Am. Chem. Soc.* **2003**, *125*, 9584.
(8) Haruta, M. *Catal. Today* **1997**, *36*, 153.
(9) Guzman, J.; Gates, B. C. *J. Phys. Chem. B* **2002**, *106*, 7659; *J. Am. Chem. Soc.* **2004**, *126*, 2672.
(10) Valden, M.; Lai, X.; Goodman, D. W. *Science* **1998**, *281*, 1647.
(11) Carrettin, S.; Concepción, P.; Corma, A.; López-Nieto, J. M.; Puntes, V. F. *Angew. Chem., Int. Ed.* **2004**, *43*, 2538.
(12) Hutchings, G. J. *Gold Bull.* **2004**, *37*, 3.
(13) Guzman, J.; Carrettin, S.; Corma, A. *J. Am. Chem. Soc.* **2005**, *127*, 3286.
(14) Fu, Q.; Saltsburg, H.; Flytzani-Stephanopoulos, M. *Science* **2003**, *301*, 935.
(15) Bamwenda, G. R.; Obucki, A.; Ogata, A.; Oi, J.; Kushiyama, S.; Mizuno, K. *J. Mol. Catal. A* **1997**, *126*, 151.
(16) Milone, C.; Ingoglia, R.; Pistone, A.; Neri, G.; Frusteri, F.; Galvano, S. *J. Catal.* **2004**, *222*, 348.
(17) Hoffman-Röder, A.; Krause, N. *Org. Biomol. Chem.* **2005**, *3*, 387.
(18) Carrettin, S.; Guzman, J.; Corma, A. *Angew. Chem., Int. Ed.* **2005**, *44*, 2242.
(19) González-Arellano, C.; Corma, A.; Iglesias, M.; Sánchez, F. *Chem. Commun.* **2005**, 19990.
(20) Hashmi, A. S. K. *Gold Bull.* **2004**, *37*, 51.
(21) Biella, S.; Rossi, M. *Chem. Commun.* **2003**, 378.
(22) Prati, L.; Rossi, M. *J. Catal.* **1998**, *176*, 552.
(23) Carrettin, S.; McMorn, P.; Johnston, P.; Griffin, K.; Hutchings, G. J. *Chem. Commun.* **2002**, 696.
(24) Abad, A.; Concepción, P.; Corma, A.; García, H. *Angew. Chem., Int. Ed.* **2005**, *44*, 4066.
(25) Corma, A.; Domine, M. *Chem. Commun.* **2005**, 4042.
(26) Ito, Y.; Sawamura, M.; Hayashi, T. *J. Am. Chem. Soc.* **1986**, *108*, 6405.
(27) González-Arellano, C.; Corma, A.; Iglesias, M.; Sánchez, F. *Chem. Commun.* **2005**, 3451.
(28) Hashmi, A. S. K. *Angew. Chem., Int. Ed.* **2005**, *44*, 6990.
(29) (a) Chen, M.; Kumar, D.; Yi, C.; Goodman, D. W. *Science* **2005**, *310*, 291. (b) Hakkinen, H.; Abbet, S.; Sánchez, A.; Heiz, U.; Landman, U. *Angew. Chem., Int. Ed.* **2003**, *42*, 1297.
(30) Lemire, C.; Meyer, R.; Shaikhutdino, S.; Freund, H. J. *Angew. Chem., Int. Ed.* **2004**, *43*, 118.
(31) Pyykkö, P. *Angew. Chem., Int. Ed.* **2004**, *43*, 4412.

 **10.1021/ja057998o CCC: $33.50** 

***Scheme 1.*** Synthesis of Soluble Ligands and Homogeneous Complexes

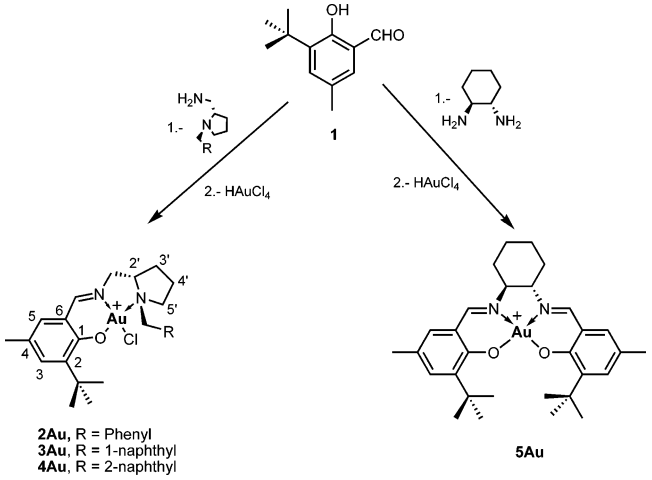


(TOFs), and by a combination of experimental and theoretical calculations[31−33] a feasible mechanism is proposed. The reaction mechanism has been studied in detail, and the energetics of each elementary step have been calculated. Theoretical calculations show the effect of the solvent on the reaction mechanism and predict that the use of polar supports should favor the activity of the homogeneous catalysts when supported on solid carriers, this being confirmed by experimental results. The presence of surface protons on the carrier increases further the activity of the catalyst, showing that the Au(III) can be as active as the corresponding Pd(II) complexes.

## Experimental Section

**Homogeneous Catalysts.** The synthesis of soluble ligands is based on the condensation of (*S*)-(*N*-benzyl-2-pyrrolidinyl)methylamine, (*S*)-[1-(1-naphthylmethyl)-2-pyrrolidinyl]methylamine, (*S*)-[1-(2-naphthylmethyl)-2-pyrrolidinyl]methylamine, and (1*S*,2*S*)-1,2-diaminecyclohexane with 3-*tert*-butyl-5-methylsalicylaldehyde in the presence of 3 Å molecular sieves.[34] Their respective Au complexes were prepared by addition of tetrachloroauric acid to an ethanolic solution of ligand; one chloride anion was displaced by the phenolic anion while the amine and imine nitrogens were coordinated with the metal in a square planar arrangement (Scheme 1). The complexes precipitated in EtOH were obtained as microcrystalline stable solids, soluble in organic solvents, with high purity and yields. The structure of all the complexes was confirmed by elemental analysis (C, H, N, and Au), by IR, $^{1}$H, and $^{13}$C NMR spectroscopies, and by electrospray mass spectrometry.

**Heterogenized Catalysts.** Au(III) complexes were prepared on all-silica and silica−alumina MCM-41,[32] as well as on pure silica ITQ-2 supports.[35] All solids were functionalized in the same manner according to the procedure showed in Scheme 2.

Supported precursors **1−(support)** were obtained by refluxing in toluene for 16 h a mixture of 3-*tert*-butyl-5-methylsalicylaldehyde and the respective support. These anchored aldehydes reacted with an equimolecular amount of the respective amine to afford the supported Schiff base ligands, **2−5−(support)**, as fine powdered solids. These materials were characterized by microanalysis, FTIR, and $^{13}$C NMR. The heterogenized ligands were reacted with tetrachloroauric acid to give the corresponding anchored gold complexes.

**Catalytic Experiments.** In a typical experiment the reaction was carried out in a 100 mL autoclave at 40 °C, 4 bar of $H_2$, and 1/1000 metal-to-substrate molar ratio with ethanol as solvent. The evolution of the hydrogenated products with time was monitored by GC with a glass capillary column (methylsilicone (OV-1701)) and methylsilicone−heptakis[2,3-dipentyl-6-(*tert*-butyldimethylsilyl)]-$\beta$-cyclodextrin.

**Computational Details.** Calculations were carried out using the program package Gaussian03[36] at the density functional theory (DFT) level by means of the hybrid B3LYP functional.[37] The basic set is double-$\zeta$ for all the atoms; for the Au, the LANL2DZ[38] pseudopotential and its associated basis set for the valence electrons were used. The O and N atoms were described by the 6-31g(d) basis set; for the Cl atom additional diffuse functions were added, 6-31+g(d). For the C and H atoms directly involved in the reaction, the 6-31g(d) and 6-31g(d,p) basis sets were employed, respectively, whereas the 6-31g basis set was used for the remaining C and H atoms. For the saddle points, the existence of only one imaginary frequency was checked by means of analytical frequency calculations.

To corroborate which are the correspondent minima linked by the considered TS, normal coordinate analyses were performed on these TS structures by intrinsic reaction coordinate (IRC) routes[39] in both reactant and product directions. Additional geometry optimizations starting from the last IRC structures were carried out when the IRC calculations did not converge themselves. The reaction pathway is assumed to be the minimum energy pathway within the potential energy surface.

***Scheme 2.*** Synthesis of Heterogenized Ligands and Complexes

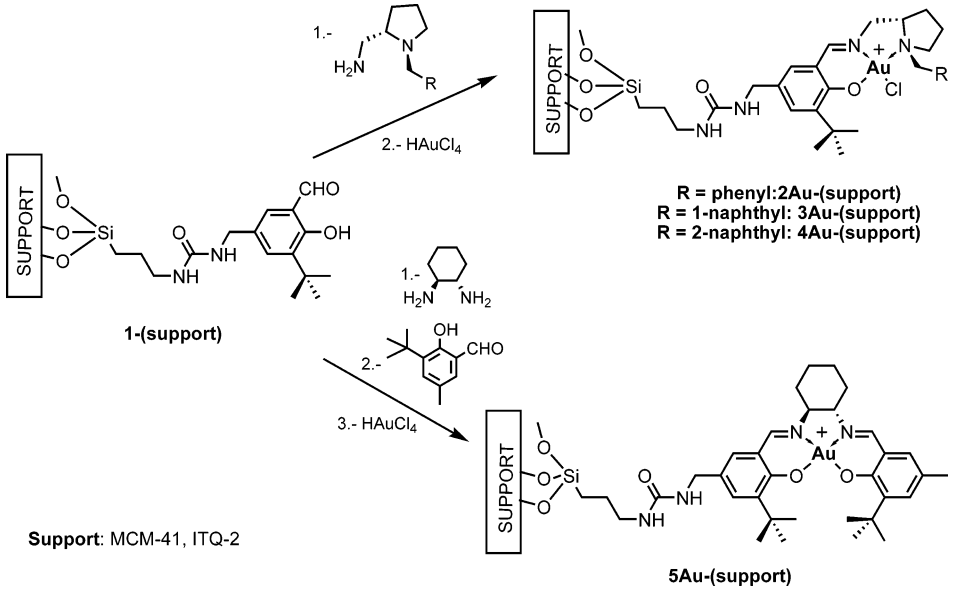

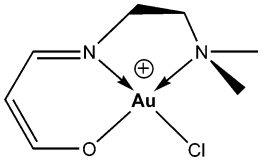


***Figure 1.*** Model complex.

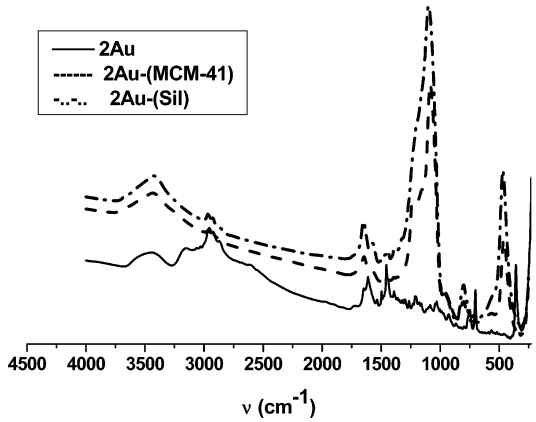


***Figure 2.*** FTIR spectra for **2Au** complexes (homogeneous and supported).

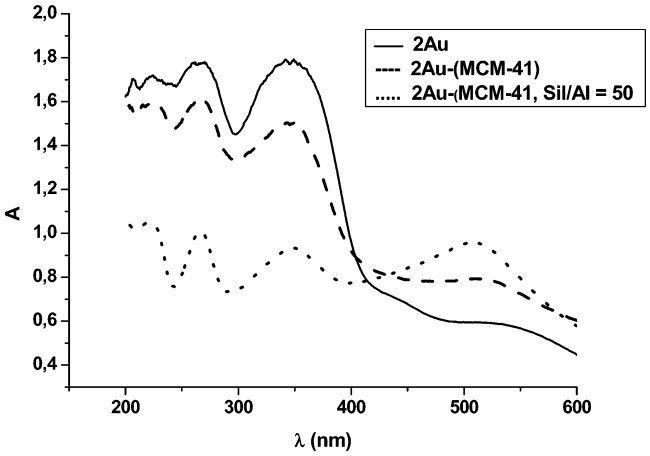


***Figure 3.*** DFTR for **2Au** complexes.

Solvent effects were included by means of the polarized continuum model[40] (PCM). The olefin selected for the theoretical calculations is ethene since it is the simplest alkene. Concerning the catalyst, calculations were performed on a complex that serves as a model for catalysts **2**, **3**, and **4**, as labeled in Scheme 1. The model complex is depicted in Figure 1.

## Results and Discussion

The nature of the complexes was verified by various spectroscopic techniques. Thus, FTIR spectra of the Au(III) complexes (see Figure 2) are characteristic of the binding of imine nitrogen. The 1600 $cm^{-1}$ band can be assigned to C═C and azomethine C═N vibrations, shifted to lower wavenumbers (relative to the free ligands due to the N-coordination of the imine). New bands in the 500−600 $cm^{-1}$ region are ascribed to $\nu$(M−O).

The DFTR spectra for all complexes (Figure 3) were obtained in the 200−800 nm range. The complexes show several bands as intraligand $\pi \rightarrow \pi^*$, n $\rightarrow \pi^*$ transitions in the aromatic ring, azomethine group, and charge-transfer transition. The bands in the 400−450 nm region correspond to d−d transitions expected for planar complexes and metal-to-ligand charge-transfer bands. The diffuse reflectance spectra of M(ligand) complexes are almost identical before and after the heterogenization process, indicating that the complexes maintain their geometry and their electronic surrounding after heterogenization without significant distortion.

***Table 1.*** Turnover Frequencies (TOF, $h^{-1}$)[a] for the Catalytic Hydrogenation of Diethyl Itaconate in EtOH[b]

| ligand | TOF |
|---|---|
| **2** | 3 430 |
| **3** | 9 560 |
| **4** | 11 240 |
| **5** | 3 690 |

[a] TOF = mol substrate/mol catalyst·h. [b] 4 bar $H_2$, 40 °C and substrate/catalyst ratio 1000:1.

***Table 2.*** Turnover Frequencies (TOF, $h^{-1}$)[a] for the Catalytic Hydrogenation of Diethyl Itaconate in EtOH[b]

| ligand | Au(III) | Pd(II) |
|---|---|---|
| **5** | 3 690 | 3 730 |
| **5**−(MCM-41) | 10 520 | 9 730 |
| **5**−(ITQ-2) | 8 980 | 9 870 |
| **2** | 3 430 | 3 360 |
| **2**−(MCM-41) | 4 920 | 4 980 |
| **2**−(MCM-41, Si/Al = 50) | 6 730 | 6 000 |

[a] TOF = mol substrate/mol catalyst·h. [b] 4 bar $H_2$, 40 °C and substrate/catalyst ratio 1000:1.

The diamagnetic gold complexes have been characterized by $^{13}C$ NMR spectroscopy (see Figure 4 for an example). In all cases, the spectra show the simultaneous occurrence of two sets of signals which are attributable on one hand to the substituted benzaldimine entity and on the other hand to the aliphatic part of the ligand. The $^{13}C$ NMR spectra showed the signals assigned to the C═N carbon high-field shifted and $C_1$ at $\delta \sim 160$ downfield shifted, confirming that metalation has occurred.

**Catalytic Activity of Gold Complexes.** Soluble complexes **2Au**−**5Au** and their corresponding heterogenized ones have been tested in hydrogenation reactions of diethyl ethylidenesuccinates (diethyl itaconate, diethyl citraconate, and diethyl benzylidenesuccinate) under mild conditions (20−70 °C and 2−6 bar $H_2$). The results on the hydrogenation of diethyl itaconate (40 °C/4 bar $H_2$) are given in Tables 1 and 2. It can be seen that the homogeneous gold catalysts not only are active but also give the same activity as the corresponding Pd complexes. In the case of the supported catalysts, the TOFs increase with respect to the homogeneous complex, indicating that both silica mesostructured molecular sieves (MCM-41) and

(32) Kresge, C. T.; Leonowicz, W. J.; Roth, W. J.; Vartuli, J. C.; Beck, J. S. *Nature* **1992**, *359*, 710.
(33) (a) *Computational Modelling of Homogeneous Catalysis*; Lledós, A., Maseras, F., Eds.; Kluwer: Dordrecht, 2002. (b) Braga, A. A. C.; Morgon, N. H.; Ujaque, G.; Maseras, F. *J. Am. Chem. Soc.* **2005**, *127*, 9298. (c) Balcells, D.; Maseras, F.; Ujaque, G. *J. Am. Chem. Soc.* **2005**, *127*, 3624.
(34) González-Arellano, C.; Gutierrez-Puebla, E.; Iglesias, M.; Sánchez, F. *Eur. J. Inorg. Chem.* **2004**, 1955.
(35) Corma, A.; Fornés, V.; Pergher, S. B.; Maesen, Th.; Buglass, J. *Nature* **1998**, *396*, 353.
(36) Frisch, M. J.; et al. *Gaussian03*; Gaussian, Inc.: Wallingford, CT, 2004.
(37) (a) Becke, A. D. *J. Chem. Phys.* **1993**, *98*, 5648. (b) Stephens, P. J.; Devlin, J. F.; Chabalowski, C. F.; Frisch, M. J. *J. Phys. Chem.* **1994**, *98*, 11623.
(38) Hay, P. J.; Wadt, W. R. *J. Chem. Phys.* **1985**, *82*, 270.
(39) Fukui, K. *Acc. Chem. Res.* **1981**, *14*, 363.
(40) (a) Cancès, M. T.; Mennucci, B.; Tomasi, J. *J. Chem. Phys.* **1997**, *107*, 3032. (b) Cossi, M.; Barone, V.; Mennucci, B.; Tomasi, J. *J. Chem. Phys. Lett.* **1998**, *286*, 253. (c) Mennucci, B.; Tomasi, J. *J. Chem. Phys.* **1997**, *106*, 5151.

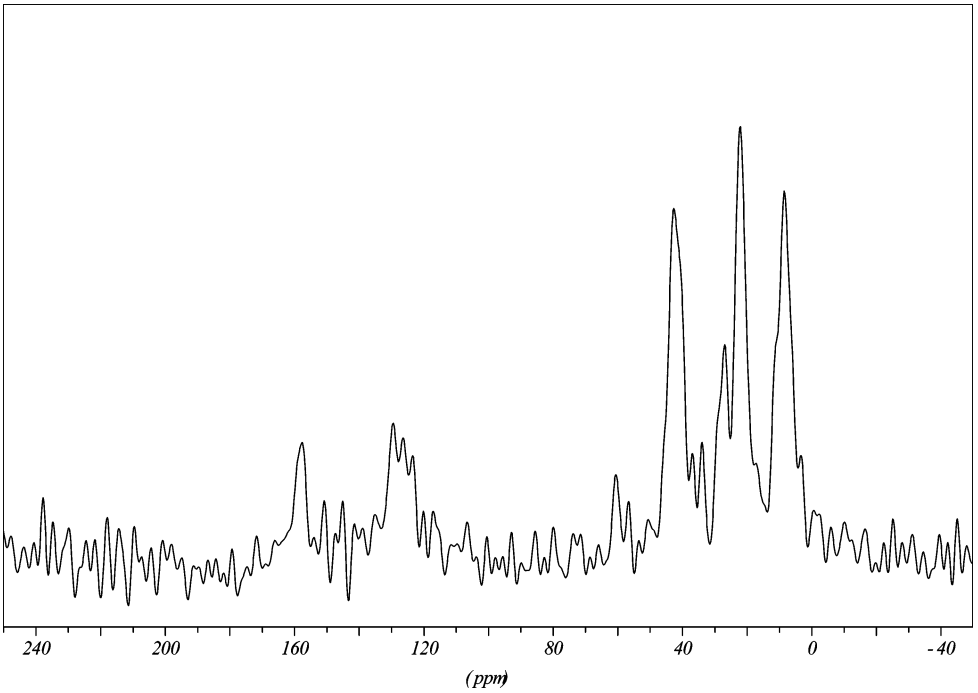


***Figure 4.*** $^{13}C$ NMR spectra of the **5Au−(MCM-41)**.

delaminated zeolites (ITQ-2) are suitable supports for heterogenizing metal complex homogeneous catalysts.

It has been shown that the introduction of acetic acid increases the rate of hydrogenation of imines by rhodium xyliphos complexes, due to the stabilization of the negatively charged transition state by the protons.[41] In our case, the introduction of surface protons in the MCM-41 support has been achieved by isomorphic substitution of Al by Si (MCM-41, Si/Al = 50). The resultant gold or Pd catalysts have a higher activity than the homogeneous or the heterogenized catalysts on the pure silica neutral supports (Table 2). These results suggest that, during the hydrogenation of imines on Au and Pd complexes, the hydrogen is activated via a heterolytic cleavage to give a hydride intermediate, which involves charge separation without any oxidative addition of hydrogen to the metal. In this case, an increase of the polarity and acidity of the support should increase the reaction rate, as has been experimentally observed (Table 2). Heterogenized catalysts are stable with time, since storage of the catalysts at room temperature for 6 months has no effect on their catalytic performance. They are also stable under reaction conditions and can be recycled at least six times without any appreciable loss in activity.

**Reaction Mechanism. (i) Activation of $H_2$.** The hydrogenation of the double bond requires the activation of molecular hydrogen by the gold complex. Two routes are known for this activation: the homolytic activation and the heterolytic cleavage of molecular hydrogen. The homolytic activation is highly improbable for the reaction system studied here due to the difficulty of the metal center to reach the oxidation number Au(V). Nevertheless, we have carried out the theoretical calculations, and the product of the oxidative addition lies ∼50 kcal/mol above reactants (in the gas phase). The barrier for this reaction will be therefore no lower than 50 kcal/mol, and consequently homolytic cleavage was rejected as a possible pathway. Thus, in the detailed reaction mechanistic study, we have considered as the first step the heterolytic cleavage of $H_2$.

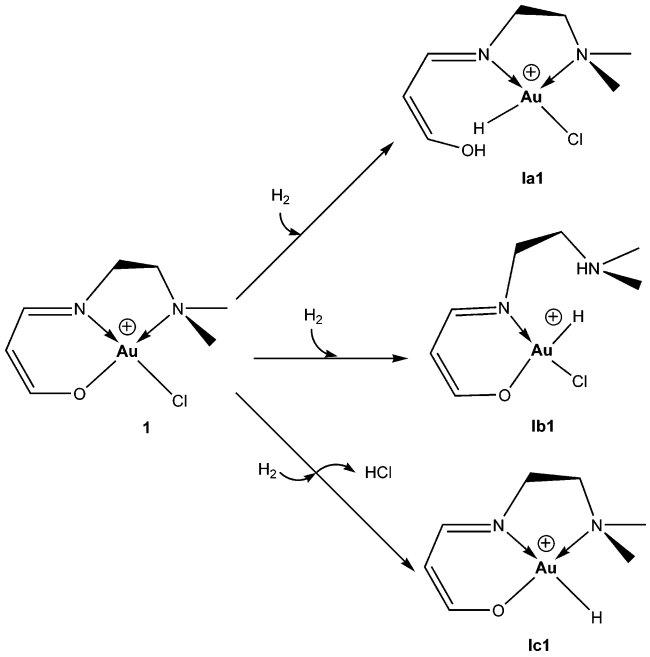


***Figure 5.*** Possible heterolytic cleavages of the dihydrogen molecule.

The $H_2$ heterolytic cleavage is more common in early transition metals, even though some cases have recently been reported for late transition metals.[42−49] For this particular system, the catalyst possesses several ligands that are potential candidates to undergo [2 + 2] $\sigma$ bond metathesis of the dihydrogen molecule: the oxygen and nitrogen of the ligand and the chlorine atom. These pathways are depicted in Figure 5.

The potential energy barriers for the direct heterolytic cleavage for each of the pathways are 47.4, 53.4, and 37.8 kcal/mol with respect to the corresponding separated reactants for the O (**tsa1**), N(amine) (**tsb1**), and Cl (**tsc1**) ligands, respec-

(41) Pugin, B.; Lendert, H.; Spindler, F.; Blaser, H. U. *Adv. Synth. Catal*. **2002**, *344*, 974.

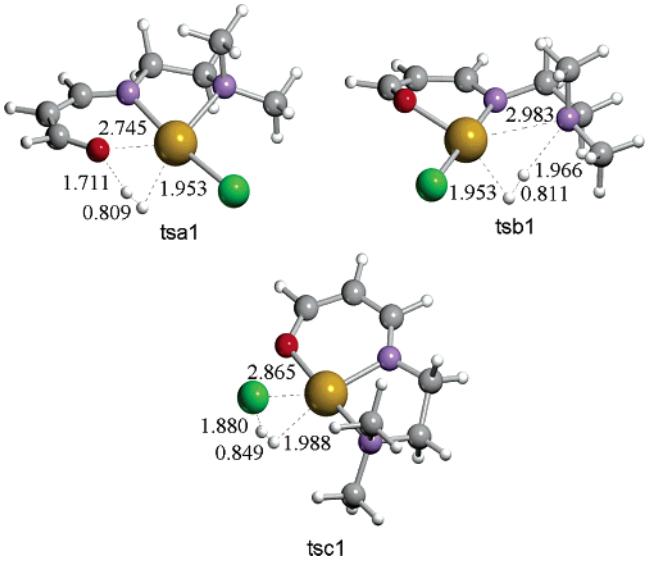


***Figure 6.*** TS of the heterolytic cleavages of the dihydrogen molecule over O (**tsa1**), N (**tsb1**), and Cl (**tsc1**). Atom colors: C, gray; H, white; Cl, green; N, purple; O, red; and Au, golden.

tively. In these pathways, the hydrogen molecule is heterolytically activated by the catalyst, and the proton goes to the ligand whereas the hydride remains bonded to the metal center. The oxidation state of the Au remains unchanged. These three transition states are similar geometrically, all of them involving a four-centered transition state with the incoming broken hydrogen molecule, the metal, and the respective ligand atom as shown in Figure 6.

The distances of the broken hydrogen are 0.809 and 0.811 Å for O (**tsa1**) and N (**tsb1**) ligands respectively, whereas in the splitting over Cl atom (**tsc1**) is slightly larger (0.849 Å). Concerning the hydride−metal bond, it follows a similar trend, with distances of 1.953 Å for **tsa1** and **tsb1** and a distance of 1.988 Å for **tsc1**. The proton−ligand distances are 1.711, 1.966, and 1.880 Å for **tsa1**, **tsb1**, and **tsc1**, whereas the heteroatom−metal distances are 2.745, 2.983, and 2.865 Å for O, N, and Cl ligands, respectively.

The barriers obtained for these processes are too high for a hydrogenation catalytic process, and we directed our efforts to search alternative pathways with lower energy barriers. It has been reported[49] that, for the heterolytic splitting of $H_2$ with related organometallic complexes, the solvent may play an active role in the reaction mechanism. By taking this into account, our attempts were focused on a six-membered-ring transition state where the heterolytic cleavage was mediated by a hydrogen-bonded ethanol molecule, since this was the solvent used experimentally (Tables 1 and 2).

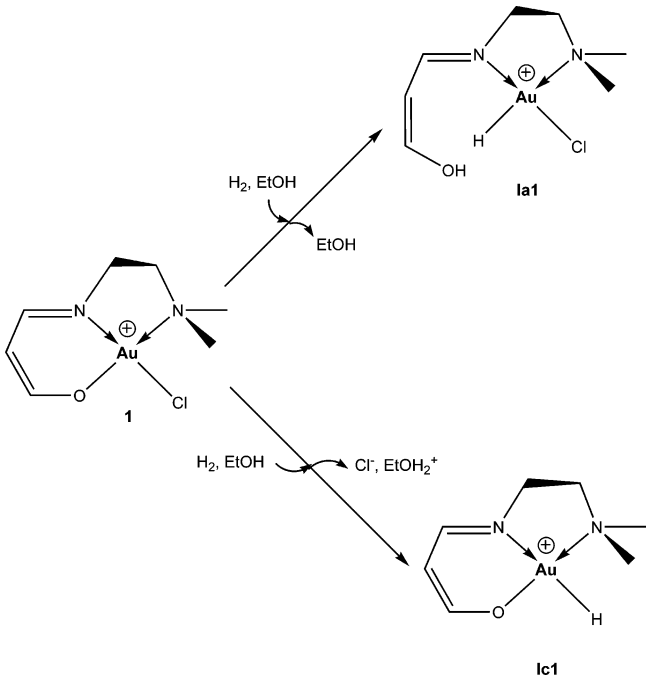


***Figure 7.*** Heterolytic cleavages of the $H_2$ assisted by a solvent molecule (EtOH) over O and Cl atoms.

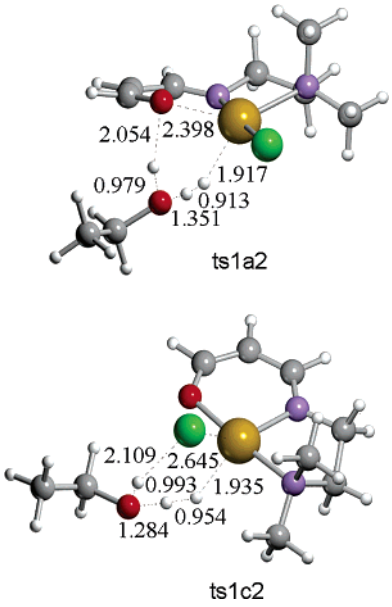


***Figure 8.*** Solvent-assisted dihydrogen heterolytic cleavage over O (**ts1a2**) and Cl atom (**ts1c2**), respectively. Atom colors: C, gray; H, white; Cl, green; N, purple; O, red; and Au, golden.

In Figure 7 are presented the two alternative pathways studied: the $H_2$ heterolytic cleavages over O and Cl ligands with ethanol assistance. The third alternative, in which the activation takes place by means of the N(amine) ligand was not considered, since the barrier for the nonassisted mechanism was the highest one and, in addition, this ligand can easily be replaced by the olefin within the catalytic cycle (vide infra).

The structures of the transition states, involving a solvent molecule, **ts1a2**, and **ts1c2**, are shown in Figure 8. The geometry of these transition states can be associated with a trigonal bipyramid structure, where the leaving ligand and the forming hydride are both at the equatorial plane. With the inclusion of the solvent molecule, the distance of the breaking H−H bond

(42) Dedieu, A.; Humbel, S.; Cornelis, J. E.; Grauffel, C. *Theor. Chem. Acc.* **2004**, *112*, 305.
(43) Niu, S.; Hall, M. B. *Chem. Rev.* **2000**, *100*, 353.
(44) Hutschka, F.; Dedieu, A.; Leitner, W. *Angew. Chem., Int. Ed.* **1995**, *34*, 1742.
(45) Hutschka, F.; Dedieu, A.; Eichberger, M.; Fornika, R.; Leitner, W. *J. Am. Chem. Soc.* **1997**, *119*, 4432.
(46) Milet, A.; Dedieu, A.; Kapteijn, G.; van Koten, G. *Inorg. Chem.* **1997**, *36*, 3223.
(47) Musaev, D. G.; Froese, R. D. J.; Morokuma, K.; Strömberg, S.; Zetterberg, K.; Siegbahn, P. E. M. *Organometallics* **1997**, *16*, 1933.
(48) Musaev, D. G.; Froese, R. D. J.; Morokuma, K. *Organometallics* **1998**, *17*, 1850.
(49) (a) Sandoval, C. A.; Ohkuma, T.; Muñiz, K.; Noyori, R. *J. Am. Chem. Soc.* **2003**, *125*, 13490. (b) Casey, C. P.; Johnson, J. B.; Singer, S. W.; Cui, Q. *J. Am. Chem. Soc.* **2005**, *127*, 3100.

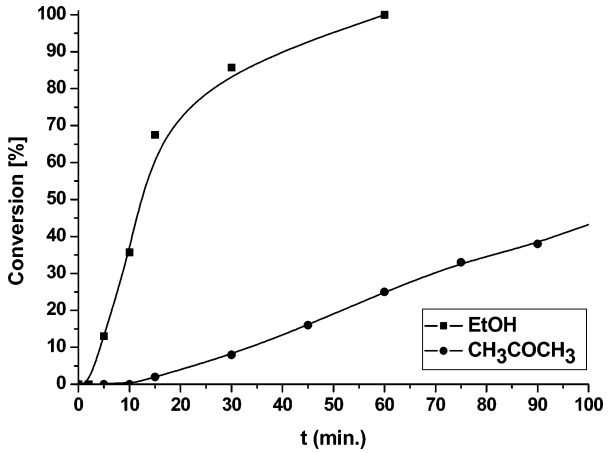


***Figure 9.*** Hydrogenation of diethyl benzylidenesuccinate under the reaction conditions given in Table 1, using two different solvents.

has been enlarged from 0.849 to 0.954 Å in the cleavage over the chlorine atom (**ts1c2)**, and from 0.809 to 0.913 Å in the splitting over the oxygen atom **(ts1a2)**. The metal−hydride distance, however, has decreased in both cases, from 1.988 to 1.935 Å in **ts1c2** and from 1.953 to 1.917 Å in **ts1a2**. Compared to the unassisted mechanism, the metal−ligand distances have decreased by 0.347 Å (2.398 Å) and by 0.220 Å (2.645 Å) for the O and Cl atom ligands.

The energies of the transition states with respect to the initial reactants are 31.5 and 26.8 kcal/mol over O and Cl, respectively, these values being much more consistent with the experimental results than those obtained for the direct heterolytic activation. The results indicate that the heterolytic cleavage of $H_2$ mediated by ethanol significantly lowers the activation barriers, decreasing those by almost 16 and 11 kcal/mol, respectively, indicating that the solvent can play a critical role in the reaction mechanism. To prove this experimentally, the hydrogenation of diethyl benzylidenesuccinate with **3Au(III)** has been carried out under the same reaction conditions but using two solvents with different proton donor ability, i.e., ethanol and acetone. The results given in Figure 9 show that, in agreement with the prediction, the initial rate of the reaction increases (the extension of the induction period decreases) when the solvent is changed from acetone to ethanol. In a more general way, these results, together with others,[49] suggest that protic polar solvents can play a determinant role in the activation of the molecular hydrogen.

The intermediate species formed after the heterolytic cleavage of $H_2$ over the O and Cl are not analogous. In the first case, the gold hydride and the EtOH molecule are formed, while the proton goes to the alkoxy ligand to form the corresponding alcohol. In the second case, besides the metal hydride, the proton goes to the alcohol molecule, forming $EtOH_2^+$ and $Cl^-$ species.

In summary, the initial activation of the dihydrogen molecule with the assistance of an ethanol molecule, forming the hydride complex, chloride, and $EtOH_2^+$ species (intermediate **Ic1a**), is the most feasible pathway to initiate the catalytic cycle.

**(ii) Coordination of the Olefin to the Catalyst.** The next step in the catalytic cycle should involve the alkene molecule. Hence, two alternative ways to coordinate the ethene molecule to the gold complex have been studied. One consists of replacing the amine of the salen ligand, giving rise to intermediate **Ic2a**, whereas the other consists of forming a five-coordinated intermediate, **Ic2bis**, with the alkene occupying the fifth coordination site. These two pathways are schematically presented in Figure 10.

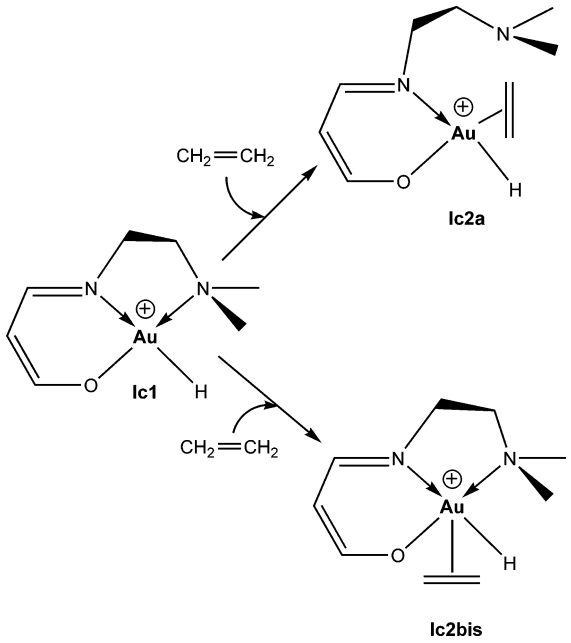


***Figure 10.*** Coordination modes of the ethene molecule.

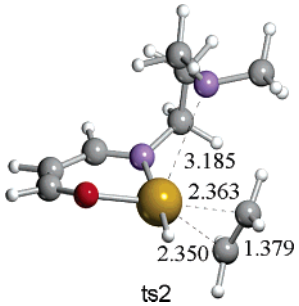


***Figure 11.*** TS for the ligand substitution of the salen aminic ligand by the incoming ethene. Atom colors: C, gray; H, white; Cl, green; N, purple; O, red; and Au, golden.

For the case where the alkene replaces the N(amine) of the salen ligand, the metallic complex remains with a square planar structure. The transition state, **ts2**, is quite product-like, with distances between the carbon atoms of the ethene and the gold atom of 2.350 and 2.363 Å, respectively (Figure 11). The Au−N bond is practically broken, with a distance of 3.185 Å. The energy of the transition state, **ts2**, for this ligand replacement is 9.3 kcal/mol, whereas the intermediate, **Ic2a**, lies 8.0 kcal/mol above the separate initial reactants.

In a related study by Vrieze, van Leeuwen, and co-workers on the insertion reaction of CO into a Pd−C bond on complexes containing terdentate nitrogen ligands, it was analogously proposed that one of the terminal N's of the chelate ligand is substituted by the incoming CO within the reaction mechanism.[50]

Comparing thermodynamically the trigonal bipyramid, **Ic2bis**, and the square planar **Ic2a**, the relative energies for these two isomers are 6.7 and 8.0 kcal/mol, respectively. Nevertheless, the energy of the transition state to obtain the pentacoordinated structure is 22.2 kcal/mol, above the energy of the separate

(50) Groen, J. H.; Zwart, A. D.; Vlaar, M. J. M.; Ernsting, J. M.; van Leeuwen, P. W. N. W.; Vrieze, K.; Kooijman, H.; Smeets, W. J. J.; Spek, A. L.; Budzelaar, P. H. M.; Xiang, Q.; Thummel, R. P. *Eur. J. Inorg. Chem.* **1998**, 1129.

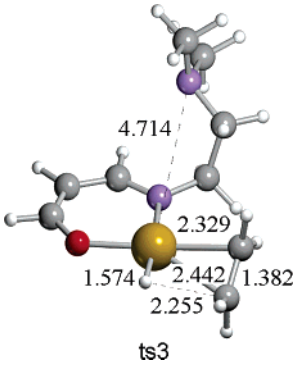


***Figure 12.*** TS of the insertion process of the ethene molecule into the Au−H bond. Atom colors: C, gray; H, white; Cl, green; N, purple; O, red; and Au, golden.

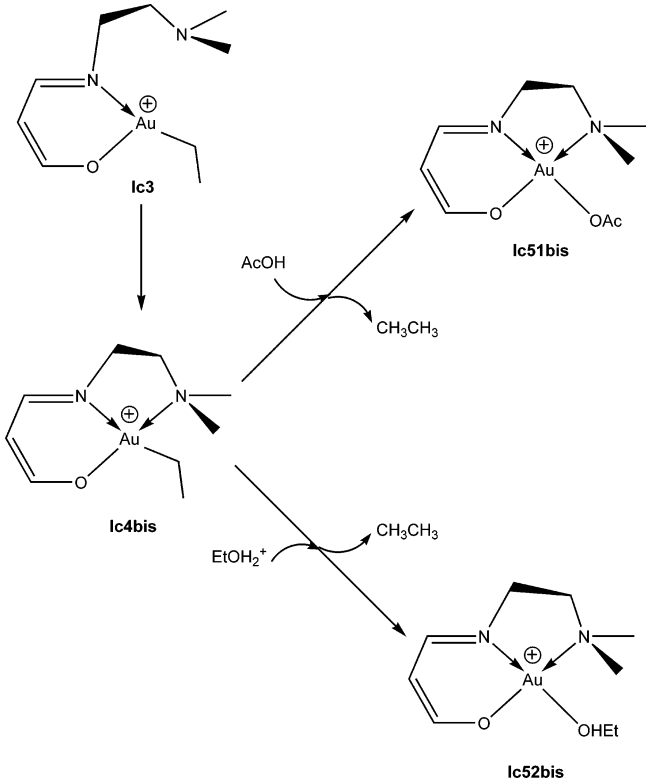


***Figure 13.*** Different protonation processes depending on the protonating agent.

reactants. Thus, the energy of the transition state within the potential energy surface is much lower than that obtained for the formation of the pentacoordinated structure (9.3 vs 22.2 kcal/mol). Hence, according to these results, the pathway going through a trigonal bipyramidal structure is less energetically favorable by 12.9 kcal/mol than that involving a square planar structure where the aminic N is not coordinated to the metal.[50]

The difference between **Ic2a** and the next intermediate, **Ic2b**, is a rotation of the lateral chain of the aminic N ligand (0.9 kcal/mol), the coordination of the olefin in both cases being perpendicular to the plane containing the metal center and the other ligands.

Once the olefin is in the coordination sphere of the catalyst, the following step corresponds to the insertion of the alkene into the Au−H bond. The energy of the formed intermediate, **Ic3**, is −2.0 kcal/mol. The **ts3** structure (see Figure 12) involves the rotation of the olefin concomitantly to the insertion process

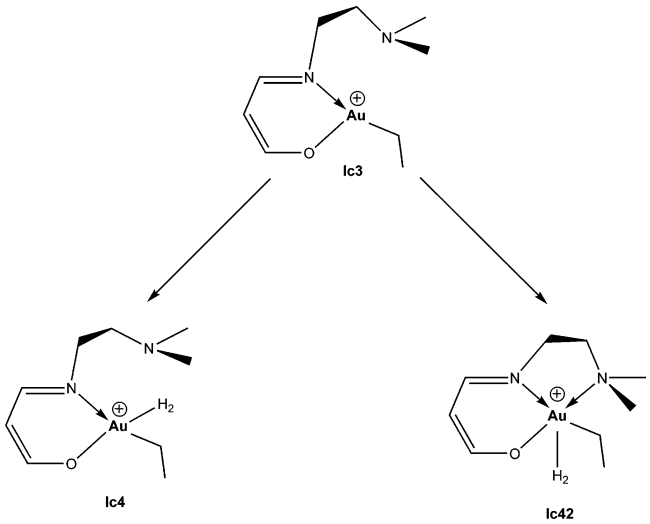


***Figure 14.*** Coordination modes of the dihydrogen molecule.

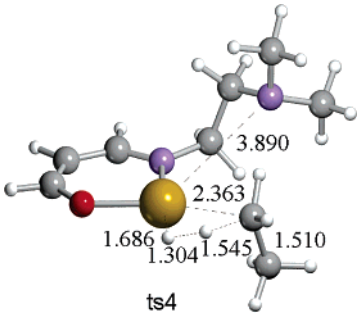


***Figure 15.*** TS of $H_2$ hydrogenolysis to close the catalytic cycle. Atom colors: C, gray; H, white; Cl, green; N, purple; O, red; and Au, golden.

itself. The forming C−H bond is 2.255 Å, and the associated barrier is around 4 kcal/mol.

**(iii) Closing the Catalytic Cycle.** The next step in the reaction mechanism corresponds to the second hydrogenation process. At this point, several hydrogen sources have been considered: a proton donor present in solution, like an acid (AcOH), a protonated solvent molecule ($EtOH_2^+$, generated in the heterolytic activation of $H_2$), and the dihydrogen molecule ($H_2$).

Figure 13 shows the possible pathways when the hydrogen source is a proton donor present in solution. In this case, we considered that the N(amine) of the salen ligand coordinates to the vacant site to form the **Ic4bis** intermediate. This process is exothermic by 37.2 kcal/mol. The reaction between **Ic4bis** and AcOH gives rise to the **Ic51bis** intermediate and the ethane products. The energy barrier for this process is 57.5 kcal/mol, which is too high for the reaction to proceed through this mechanism. In a similar way, using ethanol (the solvent itself) as a proton donor, the barrier will be even higher due to the lower acidity of ethanol.

We have also considered a protonated solvent molecule ($EtOH_2^+$), which is the strongest acid species in an ethanol solution, as a proton donor. This species may be generated in the initiation step after the heterolytic cleavage of a $H_2$ molecule, or from the addition of acetic acid to the reaction media. The energy barrier for this process, which generates the intermediate **Ic52bis**, is 37.5 kcal/mol. Though lower than in the previous case, this is still too high to be acceptable within the reaction mechanism.

Given the fact that these two species explored as proton donors give very high energy barriers, we have considered an

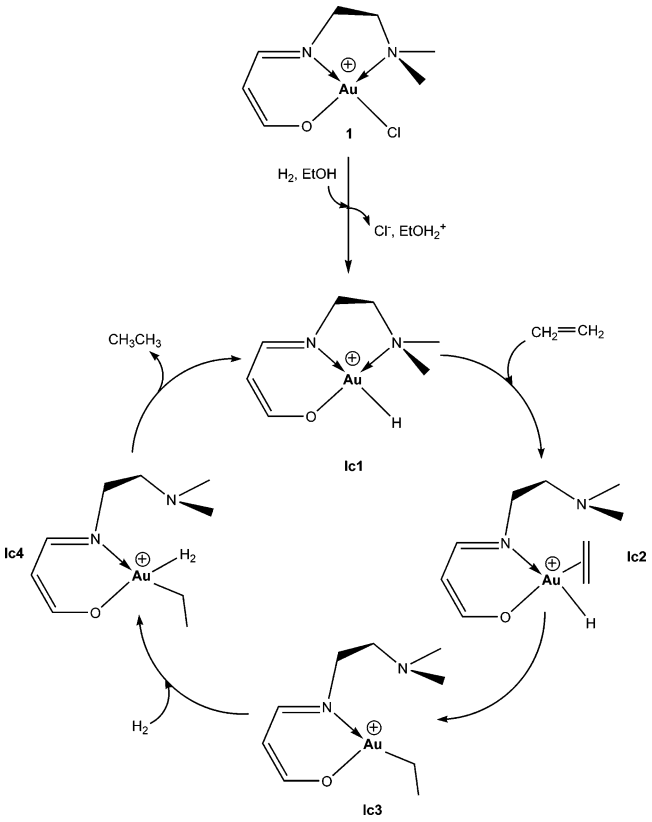


***Figure 16.*** Proposed catalytic cycle.

alternative pathway where the proton source is the dihydrogen molecule. For the coordination of the $H_2$ into the intermediate **Ic3**, there are two alternatives: a process where the dihydrogen molecule coordinates into the vacant site of intermediate **Ic3** to form intermediate **Ic4**, or a process where the N(amine) of the salen ligand coordinates to the vacant site (**Ic4bis**), and after that the $H_2$ molecule coordinates to the complex, forming a pentacoordinated complex, **Ic42** (see Figure 14).

Extensive investigation of the energy potential surface around the coordination mode for **Ic42** intermediate was performed with no success, suggesting that if this intermediate exists, it will be very high in energy.

The analysis of the other alternative pathway, in which the $H_2$ molecule coordinates to the vacant site, shows that the energy of the **Ic4** intermediate is −2.9 kcal/mol. Once $H_2$ is coordinated, the next step should correspond to hydrogenolysis, giving both the regenerated hydride−metal catalyst and the final product, ethane (**Ic1c**). The $H_2$ activation proceeds via a four-centered metathesis-like transition state (**ts4**, see Figure 15), which is characterized by a highly dissociated H−H bond (1.304 Å). The Au−H bond-forming distance is 1.686 Å, whereas the C−H bond-forming distance is 1.545 Å. Although the Au−N distance is quite long (3.890 Å), the aminic N atom ends up coordinating to the metal center, and therefore regenerating the catalyst.

The barrier for this step, 15.0 kcal/mol, is not very energetically demanding and provides an elegant and easy way of closing the catalytic cycle. An analogous hydrogenolysis step has also been proposed by Morokuma, Musaev, and co-workers in diimine−nickel-catalyzed ethylene polymerization.[51]

**The Global Reaction Mechanism.** The complete catalytic cycle, simplifying the steps which involve conformational rearrangements, is shown in Figure 16. The corresponding energy profile for the complete catalytic cycle is shown in Figure 17.

In the proposed catalytic mechanism, the highest energy barrier corresponds to the heterolytic activation of the $H_2$ molecule, giving rise to the substitution of the chlorine by H. This should result in an induction period in the kinetic curve, which is found experimentally to be more significant at low temperature (Figure 18a) and when the steric impediment for the olefin increases (diethyl itaconate < diethyl citraconate <

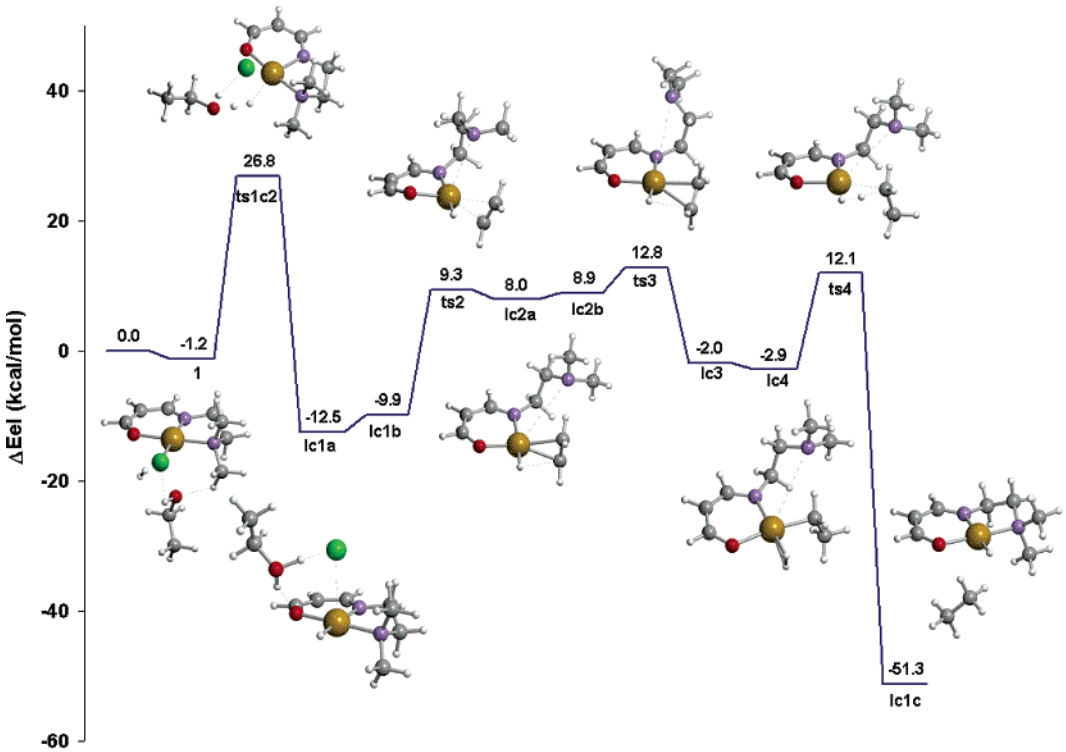


***Figure 17.*** Energy profile for the proposed mechanism. Atom colors: C, gray; H, white; Cl, green; N, purple; O, red; and Au, golden.

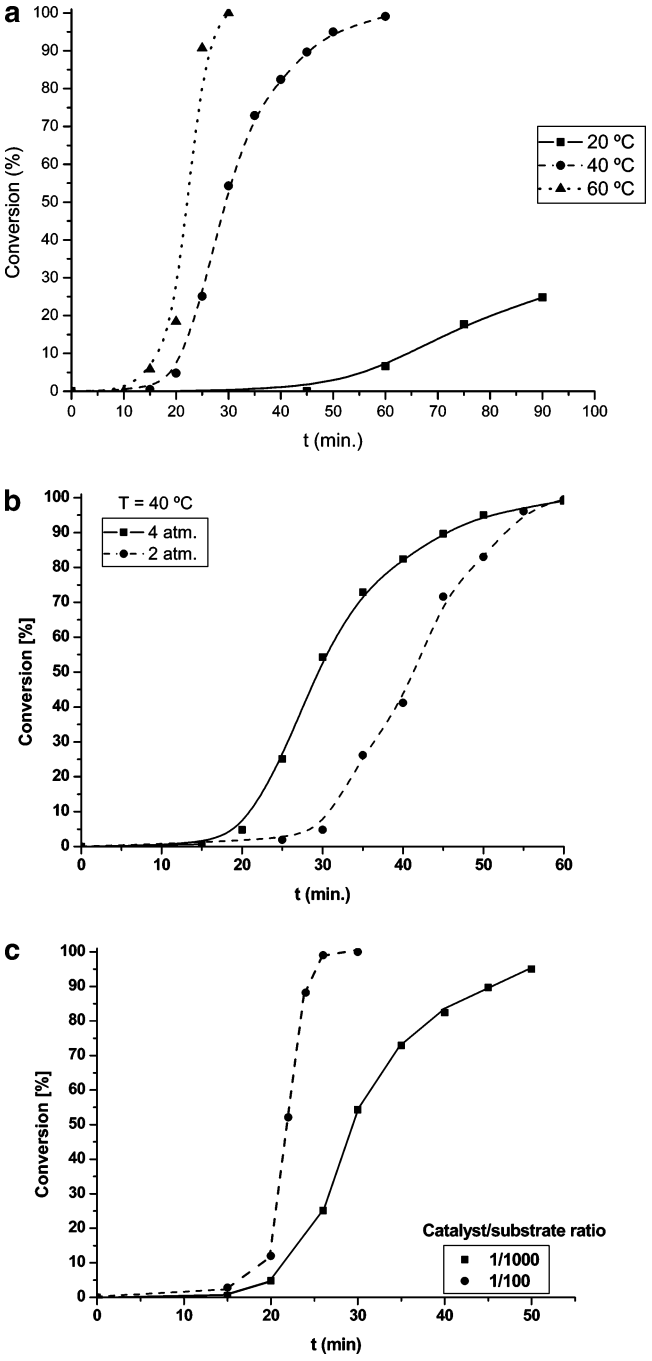


***Figure 18.*** Hydrogenation of diethyl benzylidenesuccinate using catalyst **2Au(III)** and ethanol as solvent: (a) influence of the reaction temperature; (b) influence of the $H_2$ pressure; and (c) influence of the substrate concentration.

diethyl benzylidenesuccinate). Also in agreement with this, we have seen that the induction period diminishes when the partial pressure of $H_2$ is increased from 2 to 4 bar (Figure 18b). In this step, the solvent is playing a critical role by lowering the activation barrier, as is observed experimentally (Figure 9). Also, Figure 18c shows the influence of the substrate concentration on the kinetic profile.

The hydrogen molecule only has to be initially activated by means of solvent-assisted heterolytic cleavage. After this initiation step, the activation of the $H_2$ molecule takes place in a different way within the catalytic cycle. The $H_2$ molecule coordinates to a vacant site to undergo a hydrogenolysis process.

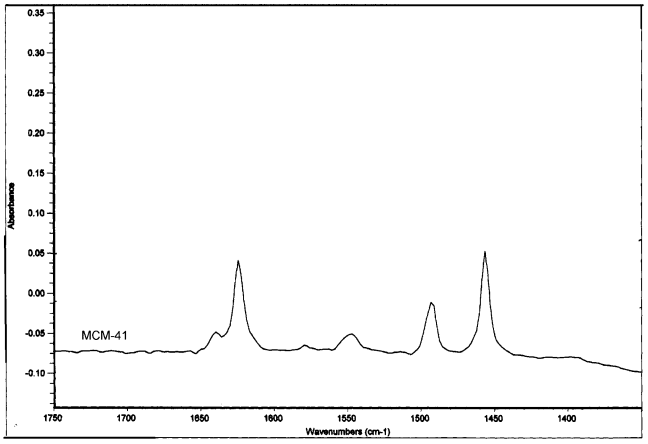


***Figure 19.*** IR spectrum of pyridine adsorbed on MCM-41, Si/Al = 50.

In such a way, the catalytic cycle proceeds much more easily. After the induction period that corresponds to the formation of species **Ic1a** (see Figures 7 and 17), the highest energy barrier step within the catalytic cycle corresponds to the inclusion of the olefin (**ts2**). In good agreement with this, we observe that, after the induction period, the rate of the reaction increases with increasing olefin concentration up to a value in which saturation of active sites occurs and the pseudo-order of the reaction becomes zero with respect to the olefin.

The activation energy for the olefin insertion step calculated theoretically is in the order of 19 kcal/mol. If we calculate to a first approximation the apparent activation energy from the reaction rate corresponding to the conversion data at different temperatures given in Figure 18a for the hydrogenation of diethyl benzylidenesuccinate, a value of ~10 kcal/mol is obtained, which is in the range of values found very often for alkene hydrogenation.

**Enhancing Catalytic Activity by Supporting the Homogeneous Catalysts: Lessons from the Theoretical Study.** From the theoretical study on the reaction mechanism for hydrogenation of olefins with the gold catalyst, it was concluded that the solvent plays an important role. Furthermore, the presence of proton donor species can also be positive for the reaction to occur. Then, if this is the case, it may very well be that, by supporting the homogeneous gold complex on a polar support, its activity can increase instead of decreasing as generally occurs when supporting metal complexes on solid carriers. Furthermore, if protons are generated on the surface of the support, this can have a further positive catalytic effect, as explained in previous sections. To test these hypotheses, we have supported Au(III) complexes **2** and **5** on pure silica MCM-41 and ITQ-2, whose surfaces have many silanol groups (very polar supports), as well as on MCM-41 in the form of aluminosilicate that presents surface Brönsted acid sites.[52] All solids were functionalized in the same manner according to the procedure showed in Scheme 2. The heterogenized complexes were also characterized by spectroscopic and analytical methods, and they remain unaltered after the heterogenization process, as can be seen in Figures 2 and 3.

The catalytic results presented in Table 2 clearly show an increase in TOF when Au(III) complexes **2** and **5** are supported on the two high surface polarity carriers. In the case of ligand

(51) Musaev, D. G.; Froese, R. D. J.; Svensson, M.; Morokuma, K. *J. Am. Chem. Soc.* **1997**, *119*, 367.
(52) Corma, A. *Chem. Rev.* **1997**, *97*, 2373.

**2**, this has also been supported on the corresponding aluminosilicate (ratio Si/Al = 50) of the MCM-41 that presents Brönsted acidity, as demonstrated by pyridine adsorption. Indeed, the IR spectrum of pyridine adsorbed on the MCM-41 (Si/Al = 50) shows, after desorption at 150 °C in a vacuum to remove the physisorbed pyridine (Figure 19), a band at ~1545 $cm^{-1}$ that corresponds to the pyridinium ion formed by protonation of pyridine by surface Brönsted acid sites. The results in Table 2 indicate that the presence of surface acidity further increases the activity of the catalyst owing to the stabilization of the charged transition state.

It is worth mentioning that the gold complexes have an activity similar to those of Pd (see Table 2), the effects of the support being very similar. This can be an indication that the hydrogenation proceeds through a similar mechanism on both types of complexes.

## Conclusions

It has been found that Au(III)−Schiff base complexes are active catalysts for hydrogenation of olefins, their activity being similar to that of the corresponding Pd complexes.

The mechanism of the reaction involves as the first step the heterolytic cleavage of $H_2$, this being the controlling step of the reaction, as demonstrated by the presence of an induction period in the kinetic curve.

In this step, the selection of the solvent plays a critical role for lowering the activation barrier. After the induction period, which corresponds to the formation of the active catalytic species, has occurred, the controlling step of the reaction is the insertion of the olefin.

It is found that, by supporting the Au(III) complexes on a high surface polarity support, the catalytic activity does not, as usual, decrease but rather increases. This increase is even larger when the surface of the carrier contains Brönsted acid sites.

Salen complexes of Au(III) give the same TOF as the corresponding complexes of Pd(II), Au(III) having the same $d^8$ electronic structure as Pd(II). The same positive effect of the support is also observed with the Pd(II) complex, suggesting that a similar mechanism of reaction should apply to the salen−Pd(II) complexes.

**Acknowledgment.** The authors thank Ministerio de Educación y Ciencia (Project MAT2003-07945-C02-01 and -02, Project CTQ2005-09000-C02-01, Ramón y Cajal contract to G.U., and FPU fellowships to A.C.-V.), the Auricat EU Network (HPRN-CT-2002-00174), and Generalitat de Catalunya (2005/SGR/00896) for financial support.

**Supporting Information Available:** Complete ref 36 and absolute energies and Cartesian coordinates. This material is available free of charge via the Internet at http://pubs.acs.org.

JA057998O